# CROSSING NUMBER BOUNDS OF MOSAIC KNOT DIAGRAMS

BY

SARAH E. ROBERTS

A Thesis Submitted to the Graduate Faculty of

WAKE FOREST UNIVERSITY GRADUATE SCHOOL OF ARTS AND SCIENCES

in Partial Fulfillment of the Requirements

for the Degree of

MASTER OF ARTS

Mathematics and Statistics

May 2017

Winston-Salem, North Carolina

Approved By:

R. Jason Parsley, Ph.D., Advisor

Hugh N. Howards, Ph.D., Chair

Jeremy A. Rouse, Ph.D.

## Acknowledgments

I would like to thank Dr. Parsley for his guidance throughout our research, and Dr. Howards and Dr. Rouse for being some of my most encouraging and inspiring professors. I also want to thank my peers for their camaraderie and collaboration, and my husband Tyrell Roberts for his support.

# Table of Contents

# List of Figures

# Abstract

Sarah E. Roberts

In this thesis, we tabulate some previously undocumented link mosaic diagrams. Next we prove an upper and lower bound on crossing number of certain mosaic diagrams of knots in terms of winding number for knot diagrams that make only counterclockwise turns. Next we begin drawing mosaic diagrams that have a more grid-like structure and no crossings. This grid structure of a knot is similar to a "grid diagram" which is equivalent to the arc presentation of a knot diagram. We generate grid diagrams using pairs of permutations from the group $((S_{n-1} \times S_n)$. These permutations form a set of coordinate pairs that locate the position of a turn tile in the diagram.

# Chapter 1: Introduction

Knot theory, although a recent focus of mathematical study, has a rich history. Knots themselves have been used practically and artistically much longer than they have in any mathematical context. Since the mathematical focus of knot theory began, there have been many developments and discovered applications to the study of knots. Applications of knot theory have been found in statistical mechanics, particle physics, astronomy, molecular biology, and chemistry. The search for knot invariants has inspired a great deal of creativity in the field. Because knot invariants can help us differentiate between knots there is a lot of motivation to find new invariants. This search has led to drawing knots with sticks, coloring diagrams, polynomials have been made to describe them.

We begin our study of knots in Chapter 2. We discuss helpful concepts, theorems, and definitions that will be used throughout the duration of our work. After reading "Knot Mosaic Tabulation" by [5] we noted that mosaic diagrams of knots have been tabulated for small crossing numbers, while mosaics for links have not been well studied. So in Chapter 3 we tabulate mosaic diagrams of links and prove mosaic number of all prime links with six or fewer crossings.

After tabulating link mosaics we began to explore diagrammatic bounds on crossing number in terms of winding number. We prove such bounds for a special type of knot diagram in Chapter 4. Next we focused on exploring a type of diagram for knots and links called a right angle diagram. These diagrams may be specified by a pair of permutations. We discuss right angle diagrams, and their direct relation to grid diagrams and arc presentations in Chapter 5.

# Chapter 2: Background

## 2.1 Preliminaries on knots and links

We will begin our work with a few definitions starting with some of our more basic terms like knot, link, and crossing number.

**Definition 1.** *A* knot *is defined as the embedding of a circle into* $\mathbb{R}^3$.

Knots and links are very similar, but have key differences. These differences can be seen in the definition below.

**Definition 2.** *A* link *is the disjoint embedding of one or more circles into* $\mathbb{R}^3$. *These closed curves may have split components or have intertwined components.*

Note that the term link encompasses the definition of a knot as well. When referring to link, we mean a knot or a multicomponent link and not explicitly a link with more than one component. When we refer to a knot however, we are always referring to a one component closed curve as defined in Definition 1. The embedding of the knot can be represented by what we call diagrams and projections of the knot.

**Definition 3.** *A knot or link* diagram *is a representation of the link in* $\mathbb{R}^2$.

**Definition 4.** *The* projection *of a knot is defined the two dimensional representation of the three dimensional knot.*

There are infinitely many projections and diagrams of knots and links. Some of these projections and diagrams may seem distinct, but all represent the same knot. These different projections and diagrams are generated by ambient isotopies, or movements of the knot that do not include cutting or gluing of the strands. The

distinct diagrams and projections may seem inherently different, for example they may have different crossing numbers, but we can always use ambient isotopies to move from one diagram or projection to another.

**Definition 5.** *A* crossing *of a knot or link is defined as a place where the strands of a knot or components of a link pass over one another, they are are portrayed in a diagram of a knot or link as a strand with two broken strands placed on either side of the whole strand.*

A diagram of a crossing is shown below in Figure 2.1.

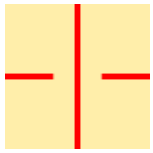

Figure 2.1: A crossing in a knot drawn as a strand with a "broken" strand underneath.

In our work we will also refer to the term knot or link "shadow" defined below.

**Definition 6.** *The* shadow *of a knot or link is a diagram of a knot or link shown as if a light were shining above the projection of the knot in* $\mathbb{R}^3$ *onto* $\mathbb{R}^2$*. Knot and link shadows are comparable to knot and link diagrams that do not have defined crossings.*

We have mentioned the crossings of knots and links quite frequently already, but we have not yet defined crossing number. It is defined as follows:

**Definition 7.** *The smallest number of crossings found across all diagrams of the knot or link is defined as the* crossing number*.*

Crossing number is an example of a link invariant, which is an important quality of a link that we define below.

**Definition 8.** *A* link invariant *is a property of a knot or link that does not change when the projection of the knot is changed under ambient isotopy.*

A link invariant can be used to tell the difference between two knots or two links. Just as crossing number of a link is an invariant, so is the mosaic number, which is an invariant derived from the mosaic diagram of the link.

**Definition 9.** *The* mosaic diagram *of a knot is the smallest $n \times n$ board on which a knot or link can be made of the square tiles, shown in Figure 2.2.*

**Definition 10.** *The* mosaic number *of a knot or link is defined as $n$ where the mosaic diagram from Definition 9 of the link is size $n \times n$.*

Unlike the artistic form of the mosaic in which pictures are made from an unlimited number of distinct tiles, we are limited to only using five distinct tiles. These tiles can be rotated by any multiple of $\frac{\pi}{2}$ radians. The tiles and their distinct rotations are shown below in Figure 2.2.

Figure 2.2: Mosaic tiles and their distinct rotations.

We form the diagram of a knot by aligning the tiles so that a *connection point* on the sides of each tile are paired with another connection point.

**Definition 11.** Connection points *are the points where the knot segments touch the edge of the tile.*

In particular, connection points are found at the midpoint of two or more edges of each tile. We use these points to *suitably connect* the tiles.

**Definition 12.** *When a mosaic is* suitably connected *there will be no unpaired connection points, and the connection points will line up to meet each other at the midpoint of the tile.*

For example, in Figure 2.4, we see a suitably connected mosaic diagram of the trefoil. Note that in order for a mosaic to be suitably connected, all crossing tiles must be contained in the *interior* of the mosaic.

**Definition 13.** *We define the* interior *of a mosaic board as the* $(n-2) \times (n-2)$ *square in the center of the* $n \times n$ *mosaic.*

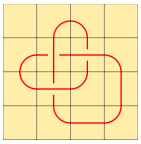

Figure 2.3: Mosaic of a trefoil knot, $3_1$.

Using enough tiles and a large enough mosaic board we can create any knot or link. This is because there are a finite number of crossings for each link, and we can always find a finite interior board that will contain these crossings so that they are suitably connected. Once we place the crossings in the interior we can connect them with the non-crossing tiles appropriately, possibly extending the interior, until we have created a diagram of the knot. Each knot can be made using a finite number of tiles, and given a sufficient number of tiles we are guaranteed to create a diagram of the knot. Note that once we have created a mosaic diagram of a knot it is easy to make the diagram as large as we desire; the more interesting and challenging task is finding the smallest board containing the knot. Once we have found this minimal mosaic, then we have found the mosaic number of the knot. For example, in Figure 2.3 we show a minimal mosaic diagram for a trefoil. We can prove that this is the

smallest diagram of the trefoil and consequently show that the mosaic number of the trefoil must be four.

**Proposition 2.1** *The mosaic number of the trefoil is four.*

*Proof.* The crossing number of the trefoil is three. We mentioned above that all crossings must be contained in the interior of a mosaic board. Thus we must have an interior that can contain at least three tiles. It is easy to see that the smallest board with at least three interior tiles must be the $4 \times 4$ board (which has an interior board of size $(2 \times 2)$ giving us four interior tiles.) Finally Figure 2.3 displays the trefoil drawn on a $4 \times 4$ board. Thus this is the smallest board admitting a diagram of the trefoil and so the mosaic number of the trefoil is four. □

The mosaic number for all knots through eight crossings has been tabulated in [5]. In Chapter 3 of this paper we find and prove the mosaic number for all links tabulated in [1] through six crossings, and discuss different methods for finding and proving mosaic number.

Mosaics of knots, specifically quantum knots, were developed by Kauffman and Lomonaco in [6] to help diagram quantum systems. They claim that their quantum knot systems could be used to simulate quantum vortices, and that they could provide understanding in other related fields of quantum systems. After developing knot mosaics Lomonaco and Kauffman posed some questions regarding application of knot mosaics, both quantum ones and purely mathematical ones. For example, how does one compute the mosaic number in general? Is the mosaic number related to the crossing number of a knot? How does one find an observable, or quantum knot invariant, for the mosaic number? They also ask questions directed towards the quantum application of mosaic diagrams.

Since the creation of these diagrams, other mathematicians have studied mosaic

diagrams of knots for mathematical applications. Modifications of the mosaic diagram have been discussed. For example, Gardunoño discusses a type of mosaic tile in [4] called a "virtual mosaic tile" and elaborates on a system of virtual mosaic diagrams that result in bounds on different types of crossings. People have also explored the idea of allowing mosaics to be rectangular instead of square, and how composition of knots affects mosaic number. The study of mosaic diagrams has been a fairly recent development in topology and ongoing research continues along these and other directions.

## 2.2 Specifics on grid diagrams and curvature

Our objective was to find relations between knot invariants and the mosaic number of a knot. As we worked toward this goal we began to reduce the mosaic diagram of a knot to what we call a "right angle diagram" or RAD. Instead of using the turn tiles from mosaic diagrams, we use tiles that have sharp right angle turns. We also label the boxes with numbers so that we can easily locate which square the turn tiles are to be placed in.

**Definition 14.** *The* right angle diagram *of a knot is simply a knot drawn with right angles and vertical and horizontal lines instead of smooth curves; in other words, it is a mosaic diagram of a knot with sharpened turns.*

Creating this type of diagram allows us to view knots in a new way. We are able to show how knots can be drawn using permutations from the group $(S_{n-1} \times S_n)/\mathbb{Z}_2$, and we are easily able to deduce the curvature of a knot by counting the number of turns that the knot made. This enables us to prove bounds on the crossing number of a knot in terms of the winding number. We also find that our right angle diagrams were just another form of grid diagrams which are also very similar to mosaic diagrams.

**Definition 15.** *A* grid diagram *is a $n \times n$ grid with one $X$ and one $O$ in each row and column. We connect each $X$ and $O$ in the same row with a horizontal strand, and each $X$ and $O$ in the same column with a vertical strand. This gives us $n$ $X$'s and $n$ $O$'s, $n$ vertical strands, and $n$ horizontal strands in the whole diagram. We call $n$ the grid number.*

These grid diagrams are equivalent to another well known diagram called the arc presentation of the knot. We will define arc presentation and thoroughly discuss its relationship to grid diagrams in Chapter 5.

Next we will discuss winding number and curvature. We use winding number to define our upper and lower bounds on crossing number, and we will also discuss curvature of knots and links because of its relation to winding number. We will begin with some definitions.

**Definition 16.** *The* winding number *of an oriented polygonal knot diagram is the sum of its signed exterior angles, and can be computed as the following:* $\frac{\sum \text{ signed exterior angles}}{2\pi}$. *The winding number of an oriented link is the sum of each component's winding number.*

A diagram an exterior angle of a curve is shown in Figure 2.7, and the term is defined below.

**Definition 17.** *The* exterior angles *of a knot or link are the angles that the tangent lines makes as they move along the outside of the curve from one point on the curve to another.*

The winding number of a knot is a knot invariant directly associated with the curvature of a knot, their relationship is shown in the following theorem and definition.

**Theorem 2.1.** *(Hopf's Umlaufsatz) If $C$ is a simple closed plane curve, then $\int_C \kappa ds = \pm 2\pi$, the positive occuring when $C$ is counterclockwise and the negative occurring when $C$ is clockwise.*

**Definition 18.** *The* total curvature *for planar curves in general will have a value of $2\pi w$ where $w \in \mathbb{Z}$ is the winding number of a closed planar loop.*

We call $\kappa(s)$ the curvature function and we assume that it is parameterized by arclength, the equation for total curvature is shown below

$$\kappa_{tot} = \int_0^L \kappa(s) ds.$$

**Definition 19.** *We define* absolute curvature *for arbitrary curves as follows;*

$$\kappa_{abs} = \int_0^L \mid \kappa(s) \mid ds.$$

For mosaics curvature is much more straight forward to calculate since the only places where the knot or link curves is on turning tiles. We have that $\kappa_{abs} = t \cdot \frac{\pi}{2}$, where $t$ is the number of turns on the curve of mosaic diagrams. For some of our work we search for bounds of knots and links that only make counterclockwise turns so in this case we have that $\kappa_{tot} = \kappa_{abs}$. Next we discuss, and prove a useful lemma and proposition for curvature of planar closed curves on mosaics.

**Lemma 2.1.** *The number of turns, $t$, used in a mosaic diagram is always even.*

*Proof.* The following proof is for a knot on a mosaic diagram. Beginning at the first turn tile of the mosaic diagram we continue along a straight section of the curve until we arrive at our next turn as we continue we get farther from the first turn tile.

Because the link on our mosaic diagram is closed we know that we must return the the first tile eventually thus each tile must have a corresponding tile that sends the curve in the opposite direction. For example, the tile in Figure 2.4 sends the curve south, so our tile in Figure 2.4 will be paired with another tile in the diagram that turns the curve north. Since we can pair all of the tiles like this, we know that the

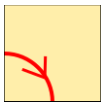

Figure 2.4: Example of an oriented turn tile.

number of turn tiles is even. This argument can be applied to each component of a link on a mosaic diagram and because sum of even numbers is still even we will have the same result for links. □

**Proposition 2.1** *For mosaics,* $\kappa_{abs} = \pi\ell$*, where* $\ell = \frac{t}{2}$*, and* $t$ *is the number of turns on the mosaic diagram.*

*Proof.* Each turn tile curves $\pm\frac{\pi}{2}$ radians, so then the absolute curvature will be $\frac{\pi}{2}t$ where $t$ is the number of turns used in the mosaic. We know that $\frac{t}{2}$ will be an integer because we showed that $t$ was even. Let $\ell = \frac{t}{2}$, then we have $\kappa_{abs} = \pi\ell$ for some $\ell \in \mathbb{Z}$. □

**Proposition 2.2** $\kappa_{abs} = \pi\ell \leq 2\pi \mid w \mid = \mid \kappa_{tot} \mid$ *when all of the turns are counterclockwise or all clockwise.* We will show this is true with two different proofs that give us different perspectives of Proposition 2.2.

*Proof.* Recall that winding number $w$, is equal to $\frac{\sum \text{ signed exterior angles}}{2\pi}$, so the greatest possible winding number for a diagram would have the value: $\frac{|t\frac{\pi}{2}|}{2\pi}$, and would be the consequence of a diagram that contained only counterclockwise (all

exterior angles measure $+\frac{\pi}{2}$ radians) or clockwise turns (all exterior angles measure $-\frac{\pi}{2}$ radians). So we have that

$$\mid w \mid = \frac{\sum \mid \text{ signed exterior angles } \mid}{2\pi} \leq \frac{\mid t\frac{\pi}{2} \mid}{2\pi} = \frac{t}{4}.$$

Now because $\ell = \frac{t}{2}$ we have that $\mid w \mid \leq \frac{1}{2}\ell$, or that

$$2 \mid w \mid \leq \ell.$$

Observe that equality holds only when all of the turns are counterclockwise. By multiplying both sides of our last inequality by $\pi$ we see that

$$\kappa_{abs} = \pi\ell \leq 2\pi \mid w \mid = \mid \kappa_{tot} \mid .$$

□

Our second proof follows from the triangle inequality.

*Proof.* Another way to derive this begins with the triangle inequality. By the definition of the triangle inequality we have that

$$\mid a \mid + \mid b \mid \geq \mid a + b \mid,$$

and we have equality if and only if $a, b$ have the same sign (i.e. $ab \geq 0$). Now let $\theta_i$ =(curvature of a particular turn $i$). For mosaics we know that $\theta_i = \pm\frac{\pi}{2}$. Since $\kappa_{tot} = \theta_1 + \cdots + \theta_{2m}$ where $2m = t$ and $\kappa_{abs} = \mid \theta_1 \mid + \cdots + \mid \theta_{2m} \mid$, we have that:

$$\begin{array}{rcl} \mid \theta_1 \mid + \cdots + \mid \theta_{2m} \mid & \geq & \mid \theta_1 + \cdots + \theta_{2m} \mid \\ \rightarrow \kappa_{abs} & \geq & \mid \kappa_{tot} \mid \end{array}$$

Note that this equality holds if and only if all turns are clockwise or counterclockwise.

□

The corollary below follows from the Proposition 2.2 above.

**Corollary 1.** *If equality holds, then* 4 *divides* $t$*, where* $t$ *is the number of turns.*

This is true because a circle can always be made of four turn pieces. All of our closed curves that contain only clockwise or counterclockwise turns will be made up of circles that are either one component, or linked.

In the following example we see this inequality for the mosaic diagram of a trefoil: the trefoil has $\ell = 4$, $t = 8$, and $w = 2$.

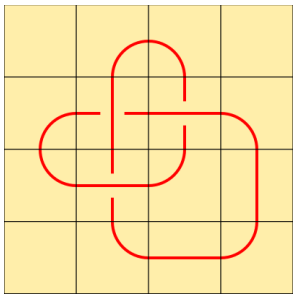

Figure 2.5: Mosaic of a trefoil knot, $3_1$.

We conclude with a more in depth look at winding number of a knot diagram since it is what we focus on when finding our bounds. Winding number can be described as the degree of a continuous mapping, or how many times a curve loops about a point inside of a curve. It is used in many different fields of mathematics, such as differential geometry, complex analysis, and topology.

Winding number of a curve can be calculated in two different ways. In the first method we consider being stationed at a point $P$, as in Figure 2.6. The winding number is the number of times the curve turns completely about $P$. In this example our curve winds about the point $P$ two times, giving us a winding number of two. For some curves however, there is no single point $P$ that will work. Consider Figure 2.6 with The second method can be used for any curve. It is done by finding the sum of signed exterior angles of the curve. We can have a positive or negative winding number depending on the orientation of the curve. Counterclockwise turns are counted as

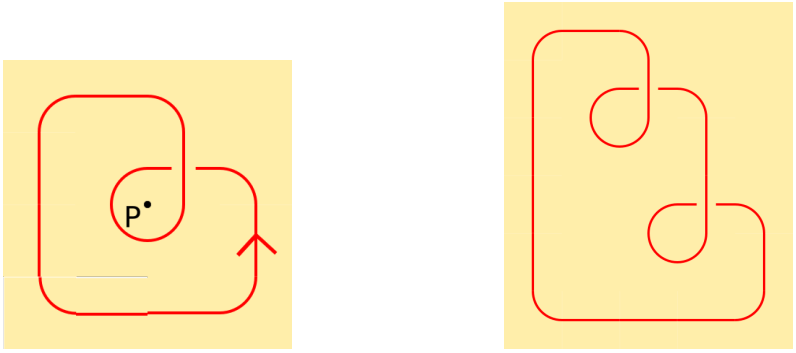


Figure 2.6: On the left we have a curve winding about a point $P$, and on the right we have a curve for which no single $P$ exists.

positive, and clockwise turns as negative. The example in Figure 2.7 shows one of the positive exterior angles that we would add to calculate winding number of this particular curve. Also note that if we start and end in the same place on a curve,

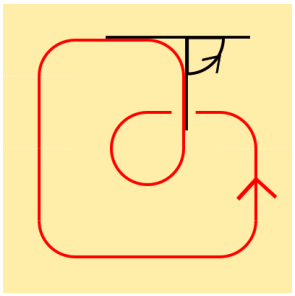

Figure 2.7: Example of an exterior angle on an oriented closed curve.

then the winding number will always be an integer. Winding number also allows us to observe something about the curve as a whole instead of only looking at one part of a curve. Now that we have explored the basic definitions and concepts from our work, we will begin our detailed work with our tabulation of link mosaics.

# Chapter 3: Tabulating with link mosaics

## 3.1 The basics for determining mosaic number

There are two approaches to finding the mosaic number of a link. In the first approach we find a mosaic of the link and then use information about the link to prove that the link cannot be made using a smaller board. Using the second exhaustive approach requires we find all possible knots and links that can be made on a board of a particular size. We continue this process, increasing the size of the board until we discover a mosaic of the link we desire. Both techniques are used in this paper to tabulate links through crossing number six. We also use several key facts in our deduction of low crossing mosaic numbers for links:

**Proposition 3.1.** *Any suitably connected mosaic board with minimal crossing number will not have a corner tile of the interior board connected to itself.*

*Proof.* Consider a suitably connected mosaic board with a corner tile that is connected to itself, as in Figure 3.1. Note that we can remove the crossing at this corner by preforming a Reidemeister I move. Because we can always reduce the crossing number by at least one, we know that any mosaic board with this attribute is not minimal. □

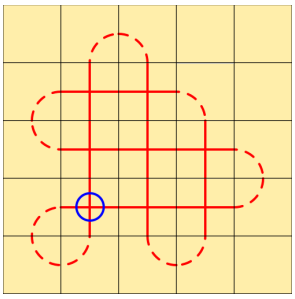

Figure 3.1: Removable crossing made by connecting a corner tile to iteslf.

**Proposition 3.2a.** *If the interior of a board has an odd number of tiles on its edge, and this edge is also made entirely of crossing tiles we can reduce the crossing number of the link by at least one.*

*Proof.* This is given to us by Proposition 3.1, and is shown below in Figure 3.2 on two edges. □

**Proposition 3.2b.** *If the interior of a board has an even edge made entirely of crossing tiles, then we can either reduce the crossing number of the projection of the knot by zero, or two.*

*Proof.* Reducing the crossing number of the diagram by zero is shown in the top of Figure 3.3. We reduce the crossing number of a mosaic diagram by two by utilizing Proposition 3.1 twice, shown in the bottom of Figure 3.3. □

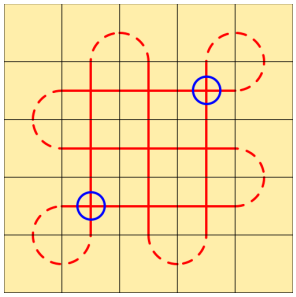

Figure 3.2: Crossings that can be eliminated on an odd board.

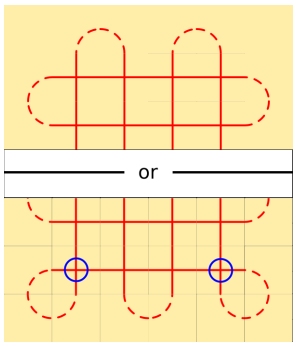


Figure 3.3: Crossings that can be eliminated on an even board.

We use these facts to rule out particular arrangements of crossing tiles in the interior. Once we have all of the possible arrangements of interior boards of a particular size, we can construct the possible links made from the interior board. This brings us to our third proposition.

**Proposition 3.3:** $(n-2)^2 \geq Cr$, where $Cr$ denotes the crossing number of a knot or link diagram displayed on the $n \times n$ mosaic board.

*Proof.* Note that if our board is of size $n \times n$, then our interior board is of size $(n-2)^2$. Then because our crossing tiles can only be placed on the interior of the mosaic diagram, the maximum number of crossings we can place is the number of interior tiles. □

## 3.2 Tabulating all links with mosaic number six and below

### 3.2.1 Finding links with mosaic number three

By drawing a circle on four tiles, is easy to see that the mosaic number of the unknot is two, and clearly this is the only link with mosaic number two. The mosaic numbers for knots through eight crossings have also been found and tabulated in [5], so we begin our work with the two component unlink, $0_1^2$. We can draw $0_1^2$ on a $3 \times 3$ mosaic by depicting both as unknots as circles that pass through the center tile as illustrated in Figure 3.4 below. Thus $M(0_1^2) = 3$. Also note that there is only one interior tile, so the maximum number of crossings that we can include is one. It is clear to see that the only one crossing link is the one component unknot, thus there are no other links that can be portrayed in a $3 \times 3$ diagram.

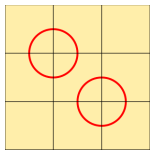

Figure 3.4: A minimal mosaic diagram of $0_1^2$.

### 3.2.2 Finding links with mosaic number four

Next we examine $2_1^2$, the Hopf link. Since the Hopf link has two crossings, its mosaic number is at least 4; Proposition 3 implies a $3 \times 3$ board contains only one tile in its interior board, so it contains at most one crossing. Now note that we can indeed draw $2_1^2$ on a $4 \times 4$ mosaic, thus $M(2_1^2) = 4$ which is shown below in Figure 3.5.

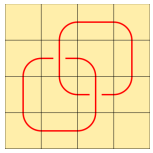

Figure 3.5: $2_1^2$

For $4_1^2$ we again see that there are 4 crossings, so we must at least use a $4 \times 4$ board. Again, we see that we can indeed create $4_1^2$ on a $4 \times 4$ board, so we have that $M(4_1^2) = 4$ shown in Figure 3.6 below. Note that we are considering the tabulated links from [1], which do not include split or composite links past $0_1^2$. If we were to consider split and composite links there would be more links to discuss with mosaic number four.

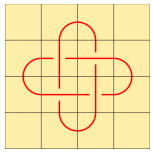

Figure 3.6: $4_1^2$

### 3.2.3 Finding links with mosaic number five

For links possessing more than four crossings Proposition 3 guarantees that we have at least mosaic number five. Since $5_1^2$ is the next link in our tabulation, and it has five

crossings we know that we must move on to the $5 \times 5$ board. We use the exhaustive second approach, discussed in Section 3.1, in order to find all possible links on a $5 \times 5$ board.

Note that we indeed have enough interior tiles to draw $5_1^2$ on a $5 \times 5$ board, and that we can draw $5_1^2$, the only five-crossing multicomponent link, on the $5 \times 5$ mosaic. So we have that $M(5_1^2) = 5$ shown below in Figure 3.7.

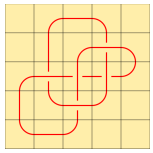

Figure 3.7: $5_1^2$

Next, we consider the possible six-crossing links in several cases and subcases. We generate cases 6A-6D by looking for valid configurations of six crossings without duplicates. We do so by considering all of the possible configurations for six crossing tiles on the interior board. For these cases we do not yet assign crossings. The subcases are created from assigning the crossings to the arrangements. Note that the bold box in the mosaic diagram encloses the interior of the mosaic, and in the top left of Figure 3.8 we show Case (6A) by only showing the interior board of the mosaic.

We begin our discussion with Case (6A). First note that there are an odd number of connection points going into the top middle boundary tile in Case (6A). We know that there are no defined tiles that have an odd number of connection points. Thus we see that this case cannot possibly make a link, and we move on to Case (6B).

For Case (6B), shown in the top right corner of Figure 3.8, we see that the green tiles are forced in order to maintain six total crossings. Any other tile choice would

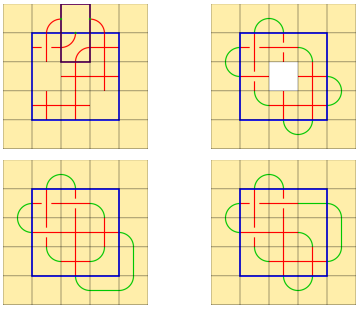

Figure 3.8: Beginning with the top left and reading from top to bottom we have cases: 6A, 6B, 6C, and 6D.

include Reidemeister I moves and reduce our crossing number by at least one. Next we have two possible choices for the center tile, and then two ways we can alternate the bottom right corner for each center tile. One choice of center tile produces the granny knot and square knot, while the other choice of center tile produces a two–component unlink, or $6_1^2$.

Next we explain how we generate our six subcases for case (6B) which are shown below in Figure 3.9. We see that in the first column we have our two different choices for the center tile without having chosen how the bottom corner alternates. The second and third columns show the two different choices for alternating the corners given the center choice.

For Case (6C), the bottom left corner of Figure 3.8, the curves drawn in the boundary tiles are forced in order to not reduce our crossing number. We have two choices for the center tile, and then four choices for alternating of the bottom corner, resulting in eight cases. These eight cases result in four trefoils, $6_2$, $6_2^*$, a two–component unlink, and $5_1$.

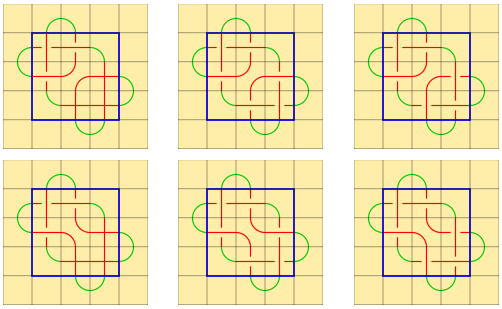

Figure 3.9: Six subcasses for case 6B.

Finally, for Case (6D) shown in the bottom right corner of Figure 3.8, we see that again the green tiles are forced, and similar to Case (6C) have eight results from the two choices of the center tile, and four choices for alternating the bottom right corner. This time we create four trefoils, $6_2$, $6_2^*$, an unknot and $5_1$.

Thus we can conclude that the only prime six –crossing multi component link that exists on a $5 \times 5$ board is $6_1^2$.

We finish finding all of the possible links on a $5 \times 5$ board by filling the whole interior with crossing tiles. The interior of a $5 \times 5$ board contains nine tiles, but by Proposition 1 we see that the largest possible crossing number on a $5 \times 5$ board is seven, shown in Figure 3.2. Now we observe all of the possible seven-crossing links on a $5 \times 5$ board. We see that in order to create seven-crossing links we must avoid creating the Reidemeister I moves described in Proposition 2. By eliminating the cases in which Proposition 2 can be applied, and the cases in which a Reidemeister II move is created we conclude that there are only four possible cases up to rotation and mirroring. These four cases are generated in the same way as the cases above. We have a choice for the center tile, and then four choices for alternating the bottom right corner. Shown below we see that Case (7A) creates the figure eight link, Case

(7B) creates $7_4$, case (7C) creates $6_1$, and finally Case (7D) creates $6_1^*$. So we see that there are no seven-crossing, two-component links on a $5 \times 5$ board.

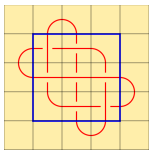

Figure 3.10: Case 7A.

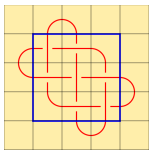

Figure 3.11: Case 7B.

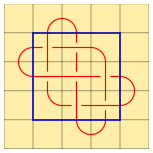

Figure 3.12: Case 7C.

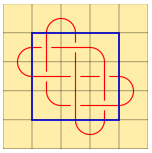

Figure 3.13: Case 7D.

We have now accounted for all possible cases of links on a $5 \times 5$ mosaic, but we still have several six-crossing links that were not found on a $5 \times 5$ board. Thus if we can draw these six-crossing links on a $6 \times 6$ diagram, then the mosaic number for this link will be 6. Note that all six-crossing links aside from $6_1^2$, which we found on a $5 \times 5$ mosaic, must fit onto a $6 \times 6$ mosaic. Thus we have that $M(6_2^2) = 6$, $M(6_3^2) = 6$, $M(6_1^3) = 6$, $M(6_2^3) = 6$, and $M(6_3^3) = 6$, all of which are shown in the table in the following section.

## 3.3 Table for links up to six crossings

Below we have a table of all of the mosaics for six crossing links:

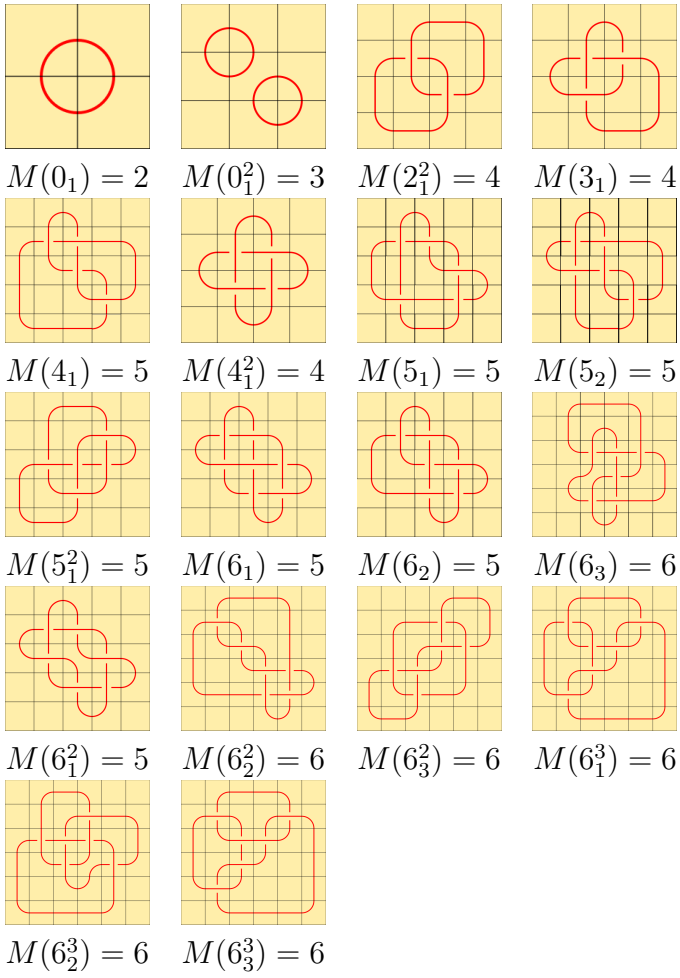

$M(0_1) = 2$ $M(0_1^2) = 3$ $M(2_1^2) = 4$ $M(3_1) = 4$

$M(4_1) = 5$ $M(4_1^2) = 4$ $M(5_1) = 5$ $M(5_2) = 5$

$M(5_1^2) = 5$ $M(6_1) = 5$ $M(6_2) = 5$ $M(6_3) = 6$

$M(6_1^2) = 5$ $M(6_2^2) = 6$ $M(6_3^2) = 6$ $M(6_1^3) = 6$

$M(6_2^3) = 6$ $M(6_3^3) = 6$

# Chapter 4: Upper and lower bounds on crossing number

## 4.1 Lower bound on crossing number

After tabulating the link mosaic diagrams, we sought bounds that could help us make better conjectures for the mosaic number for knots and links. It seemed likely that we could bound the number of crossings in a knot by the number of turns the knot made, and that this could help us estimate how large of a mosaic board we would need to make a knot. Below we prove a lower bound on crossing number.

**Theorem 4.1.** *Let $Cr(\gamma)$ be the crossing number and $w(\gamma)$ be the winding number of a closed curve, $\gamma \in \mathbb{R}^2$, that only makes $\frac{\pi}{2}$ radian counterclockwise turns. Then we have*

$$w(\gamma) - 1 \leq Cr(\gamma). \tag{4.1}$$

*Proof.* Consider a simple closed curve, $\gamma \in \mathbb{R}^2$ on a mosaic diagram, that only makes counterclockwise turns. We imagine that $\gamma$ is drawn so that all turns occur at integer points, i.e., in $\mathbb{Z} \times \mathbb{Z} \subset \mathbb{R}^2$. Let $\gamma$ have $C$ crossings. Our proof relies on classifying these into four categories of crossings that we will discuss below.

Next we resolve the crossings on the perimeter of the curve so that we can decompose our original curve into more simple types of curves. Resolving or smoothing our crossings breaks apart our one-component curve into one outer curve and inner curves that we label $\alpha_i$ for $1 \leq i \leq n$ for some $n \in \mathbb{N}$. First let $k$ be the number of crossings on the perimeter of $\gamma$. Then let $Cr(\alpha_i)$ denote any crossings the interior curves have with themselves, and $Cr(\alpha_i\alpha_l)$ denote crossings between any two distinct interior curves. Let $\delta$ be the outer zero-crossing perimeter curve that is created when

the crossings are resolved. In Figure 4.1, shown below, we see an example of resolving the crossings on the perimeter, and labeling the resulting curves accordingly using a six crossing planar curve. Having now accounted for four different types of crossings for $\gamma$ we observe that.

$$Cr(\gamma) = k + \sum_{i=1}^{j} Cr(\alpha_i) + \sum_{i>l} Cr(\alpha_i \alpha_l) + 0. \tag{4.2}$$

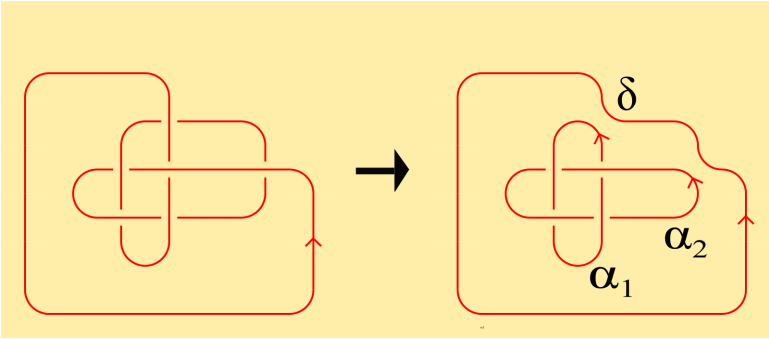


Figure 4.1: Resolving crossings in a mosaic diagram.

In general, we claim that if a curve $\gamma$ has winding number $n$, then the sum of the winding numbers of the resulting $\alpha_i$'s is $n - 1$. In order to prove this claim, we first show that resolving a crossing does not change winding number. Because we are working with $\gamma$ on a mosaic diagram we observe that crossing tiles have zero curvature (i.e., a winding number equal to zero). When we resolve a crossing tile, we replace it with a tile containing two curves. One curve on the tile has an exterior angle of $\frac{\pi}{2}$ radians, while the other has an exterior angle of $-\frac{\pi}{2}$ radians, shown in Figure 4.2 below. A crossing tile being resolved will always result with this because we must maintain the orientation of the original curves. Since the sum of the two exterior angles is zero, by definition we know that the winding number of the curves in the tile will also be zero. Thus, resolving any crossing tile will not change the winding number.

Figure 4.2: Resolving one crossing tile.

When we resolve the crossings on the perimeter we create an outer curve $\delta$ that has winding number one. Because we have shown that resolving crossings does not change the winding number of our new collection of curves, the remaining curves must have winding numbers that sum to $n-1$. In other words, given $w(\gamma) = n$, we will have $\sum_{i=1}^{j} w(\alpha_i) = n-1$, where the $\alpha_i$ denote the interior curves of $\gamma$.

This claim allows us to prove our inequality. We induct on winding number, and begin with our base case, $w = 1$.

As our base case we consider all curves with only counterclockwise turns with winding number $w = 1$. Note that the only situation in which this is true is in the class of simple closed planar curves that are oriented counterclockwise; denote this class of curves $U$. Now consider an arbitrary knot $u \in U$, then we see that,

$$\begin{aligned} Cr(u) &\geq w(u) - 1 \\ 0 &\geq 1 - 1, \end{aligned}$$

satisfying our hypothesis.

For our induction step we assume that the inequality holds true for all closed curves $\gamma$ that only make counterclockwise turns and have $w(\gamma) \leq n$. That is,

$$Cr(\gamma) \geq w(\gamma) - 1 = n - 1.$$

Now consider a closed curve $\gamma$ with only counterclockwise turns such that $w(\gamma) =$

$n+1$. We want to show that

$$Cr(\gamma) \geq w(\gamma) - 1 = n. \tag{4.3}$$

.

First note that summing the winding numbers of each individual $\alpha_i$ is equivalent to finding the winding number of the collection, or sum, of the curves: $w(\bigcup_{i=1}^{j} \alpha_i) = n = \sum_{i=1}^{j} w(\alpha_i)$. Then by our induction hypothesis $\sum_{i=1}^{j} Cr(\alpha_i) \geq \sum_{i=1}^{j}(w(\alpha_i)-1)$. Next we apply the summation to the constant term and winding number to get: $\sum_{i=1}^{j} w(\alpha_i)-j = n-j$.

We substitute this into Equation 4.2 to produce the inequality below.

$$Cr(\gamma) \quad \geq \quad k + (n-j) + \sum_{i>l} Cr(\alpha_i \alpha_l) + 0 \tag{4.4}$$

The third term, $\sum_{i>l} Cr(\alpha_i \alpha_l)$, counts the crossings between different components of the interior curves. It is greater than or equal to zero. Now we have that $Cr(\gamma) \geq k + (n-j) + 0 + 0$

Because we resolve $k$ crossings on the perimeter, k is the maximum number of interior curves that we can create. Since $j$ is the number of closed curves created in the interior we must have that $j \leq k$. So then we have that $k - j \geq 0$ which tells us that $k + n - j \geq n$. Now we rewrite Inequality 4.4 as: $Cr(\gamma) \geq k + (n-j) \geq n = (n+1) - 1 = w(\gamma) - 1$. So we have shown that Inequality 4.3 is true.

□

Now that we have shown the lower bound for crossing number in terms of winding

number it becomes natural to search for an upper bound. This is the subject of Section 4.2.

## 4.2 Upper bound on crossing number

Our next task is to find an upper bound for the crossing number of one-component closed planar right angle curves. Finding this upper bound for one-component curves is not immediately obvious, so we observe crossing numbers for $n$-component links in which each component was simple, closed, planar and only made counterclockwise turns. Note that the maximum number of times two rectangles can cross is four, this is shown in the shadow of a two component link in Figure 4.3.

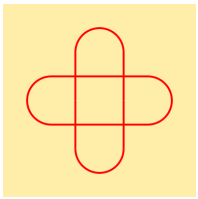

Figure 4.3: Maximum number of crossings for two simple planar closed curves.

The maximum crossing number of such an $n$-component link is easy to see when overlapping each component so that it crosses each of the other components four times, we will call such a link $L_{\max}$. An example is shown in Figure 4.4. We utilized a

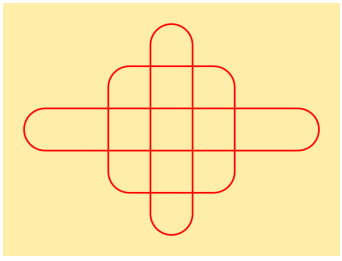

Figure 4.4: Maximum crossing three component link.

maneuver called the rectangle move, similar to "smoothing" a crossing, that combines

components of our $n$-component link to make a one-component link. Once finding the rectangle move we found that we could reverse the process with what we called the inverse rectangle move. It is easy to establish the maximum number of crossings on the $n$-component link; from this we deduce that there must be a maximum number of crossings for the corresponding one-component link.

We begin by defining the rectangle move and its inverse. First, notice that if we attempt to connect any components by breaking a straight arc of the component and then connecting the loose ends, we will create turns that are not counterclockwise, shown in Figure 4.5.

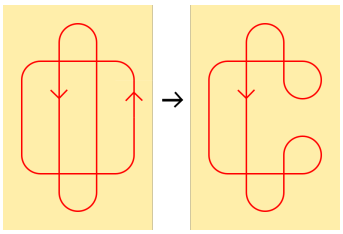

Figure 4.5: Breaking components and reattaching along straight arcs.

Since each component is only made of straight arcs, turns, and crossings, we have a limited number of places up to isotopy we can choose to break and reattach components. Because breaking components at a turn tile is isotopic to breaking a component along a straight arc, the only other place to break the a component is at a crossing. After breaking our components at a crossing we must reattach our components so that we preserve the orientation of the strands. Reattaching in this way maintains counterclockwise turns and reduces our number of components by one. We call the process of breaking two components at a crossing and then reattaching them a "rectangle move", which we define in detail below.

**Definition 20.** *A* rectangle move *combines two components of a multicomponent link*

*into one by finding a crossing shared by two distinct components of the link, and then breaking the crossing. This produces four loose ends. Reattach them to produce a single closed curve. We attach strands 1 and 2, and strands 3 and 4 to one another.*

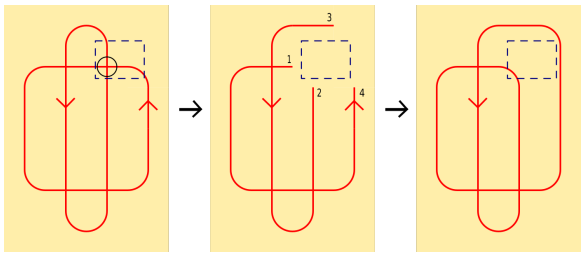


Figure 4.6: Rectangle Move shown at the circled crossing.

**Definition 21.** *The* inverse rectangle move *separates components of a one-component link using the following algorithm:*

- *We begin with our one-component closed curve $\gamma$ and find two corners that are on the same component of the link, such that the corners turn the same direction shown in Figure 4.7 (a).*

- *Next we remove the vertex of each corner, leaving four unconnected strands shown in Figure 4.7 (b).*

- *Note that there is only one way to connect the four ends that creates one additional component and maintains the orientation of the strands shown in Figure 4.7 (c).*

Performing an inverse rectangle move creates at least one additional crossing, does not change the number of turns or the winding number, and increases the number of components by one. We repeat this process until the number of components is equal

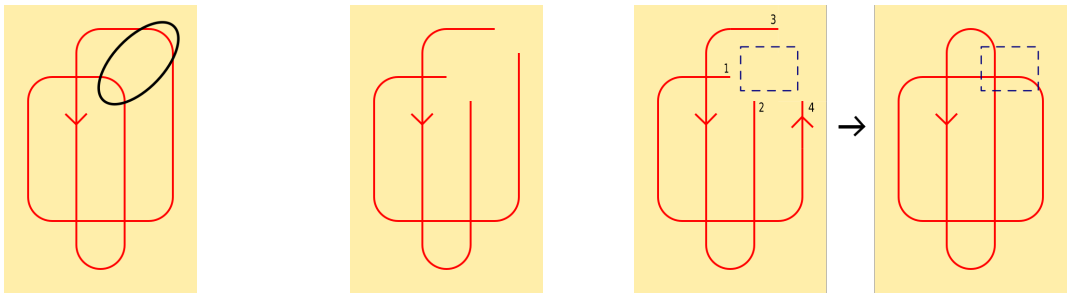


(a) Locating appropriate corner strands to apply the inverse rectangle move.

(b) Removing vertices.

(c) Connecting ends of components.

Figure 4.7: Inverse rectangle move.

to the winding number. Now we have created a link that has $w(\gamma)$ components. Since performing the corresponding rectangle moves change the $w(\gamma)$-component link into the original curve, we have shown that there is a well-defined invertible algorithm that inputs an $n$-component curve and outputs a one-component planar curve that has winding number $n$.

For our proof we want to begin with a knot diagram $D$ and produce a link $L$ that also makes only counterclockwise turns with the same winding number. Our goal is to prove the following theorem.

**Theorem 4.2.** *Let $Cr(\gamma)$ be the crossing number and $w(\gamma)$ be the winding number of a closed planar curve, $\gamma$, that only makes counterclockwise right angle turns. Then*

$$Cr(\gamma) \leq 2w^2(\gamma) - 3w(\gamma) + 1. \tag{4.5}$$

*Proof.* We begin with a knot diagram $D$, such that $w(D) = n$. Consider $L$, the $n$-component link constructed by applying $n-1$ inverse rectangle moves to $D$. Each component will be closed, simple, and planar, with winding number equal to one, i.e., a rectangle. Also note that $Cr(D)+(n-1) \leq Cr(L)$ because we used $n-1$ rectangle moves to form $L$ from $D$, and each move adds at least one crossing. Let $L_{\max}$ be the link with $n$ components as above, and maximal crossing number. Recall that such

a 3-component link was shown in Figure 4.4. Because each component has winding number one we have

$$w(L) = w(L_{\max}) = n.$$

Note that $L$ has $n$ components and recall that each set of two components can cross a maximum of four times. Now we have $Cr(L_{\max}) = 4\binom{w}{2} = 2w^2 - 2w$ where $w$ is the winding number of $L_{\max}$. Note that $Cr(L) \leq Cr(L_{\max})$ because $D$ does not necessarily have the maximum number of crossings, and $L$ is created from $D$. We previously stated that $Cr(D) + (n-1) \leq Cr(L)$. This can be rewritten as $Cr(D) + (w-1) \leq Cr(L)$ because $w = n$. So putting everything together we have

$$Cr(D) + (w-1) \leq Cr(L) \leq Cr(L_{\max}) = 4\binom{w}{2}.$$

Subtracting $(w-1)$ from both sides we have that

$$Cr(D) \leq Cr(L) - (w-1) \leq 2w^2 - 2w - (w-1).$$

Simplifying we have that $Cr(D) \leq 2w^2 - 2w - (w-1) = 2w^2 - 3w + 1$. Thus we have shown that our theorem holds, and we conclude our proof for the upper bound. $\square$

# Chapter 5: Grid diagrams and arc presentation

## 5.1 Right angle diagrams and permutations

We search for ways to generalize our bounds from Chapter 4 on crossing number to a larger category of curves. Previously we required that the diagram make only counterclockwise perpendicular turns, but we now allow both counterclockwise and clockwise 90° turns in our diagrams.

Now we will define the expanded class of planar diagrams that we consider.

**Definition 22.** *A* right angle diagram *is a closed planar curve in* $\mathbb{R}^2$ *drawn on a* $\frac{t}{2} \times \frac{t}{2}$ *grid where* $t$ *is the number of turns that the curve has. The right angle diagram is the shadow of the knot with sharp right angles instead of smooth curves for turns. The term* shadow *implies that we have not chosen crossings for the knot.*

We first consider diagrams with four perpendicular turns and find all of the possible outcomes. It is clear that that there is only one four-turn diagram up to planar isotopy, and that it is equivalent to the mosaic or grid diagram of an unknot. We continued by finding all of the diagrams that could be produced from six turns by hand. This was tedious; how could we assure that we had indeed found all of the diagrams? To do so we restructured our system of generating diagrams with $t$ turns by using a system of permutations that generated all of the possible locations on a grid where a turn tile can be found, and all of the possible ways those turns can be connected disregarding crossing assignments. We describe this process in detail below.

Note that each turn tile is connected to one vertical and one horizontal strand. Thus the total number of strands is equal to the total number of turns. Recall from Lemma 2.1 that the number of turns on a mosaic diagram is always even. Because the

only difference between a right angle diagram and a mosaic diagram is the smoothness of turns, and the crossing information, the number of turns on a right angle diagram will also be even. The number of only vertical or only horizontal strands is $\frac{t}{2}$. For simplicity, let $k = \frac{t}{2}$ so that we can write our work interns of $k$. We choose two permutations, $\phi$ from the group $S_k$, and $\sigma$ from the group $S_{k-1}$ Let $\sigma_j$ denote the $j^{th}$ column and let $\phi_i$ denote the $i^{th}$ row, then $(\phi_j, \sigma_i)$ denotes the location of the turn tile in column $j$ and row $i$. Saying $\phi \in S_k$ allows us to begin in any row. However, we require $\sigma_1 = 1$ mandating that we start in the first column of our grid. Thus $\sigma = (\sigma_1, \sigma_2, \cdots, \sigma_k)$ maybe viewed as lying in $S_n/\mathbb{Z}_n \cong S_{n-1}$.

The two permutations can be broken down into a set of "coordinate pairs" each of which denote the location of a turn tile on the RAD. Each of the numbers in $\sigma$ will be used twice in the set of coordinate pairs[1] to tell us what column to place our turn tile in, and $\phi$ will be used twice in the set of coordinate pairs to tell us the row to place our turn tile. We use $\phi$ to give the first number in the coordinate pair, and $\sigma$ to give the second number. We alternately hold one of each of the coordinates constant so that we get a vertical or horizontal segment between each turn tile. We begin by holding the $\phi$ coordinate constant first. In general we see that given permutations $\phi = (\phi_1, \phi_2, \cdots, \phi_k)$, and $\sigma = (1, \sigma_2, \sigma_3, \cdots, \sigma_k)$ our diagram would encounter turns at precisely the following coordinates

$$(\phi_1, 1)(\phi_1, \sigma_2), (\phi_2, \sigma_2) \cdots, (\phi_k, 1)(\phi_1, 1).$$

**Example 5.1.** For example the set of permutations $\phi = (231)$, and $\sigma = (132)$ give the following set of coordinate pairs

$$(2, 1)(2, 3)(3, 3)(3, 2)(1, 2)(1, 1)(2, 1).$$

This list tells us that our first point starts in the second row and the first column,

[1]This excludes the duplicate coordinate pair that sends us back to the original turn tile.

goes to the point in the second row and third column, then third row third column, third row second column, first row second column, first row first column, and finally, back to the second row and first column. Following this set of points all the way through gives us a diagram of the unknot with one crossing, shown in Figure 5.1.

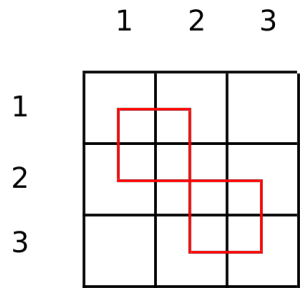


Figure 5.1: Example of drawing a knot shadow using permutations.

The ability to generate shadows of knots in this way allows us to systematically generate all ambient isotopies, rotations, and orientations of the knots with a particular number of turns. However, because we are only interested in distinct knots, generating all of the diagrams that are isotopically the same clutters our work. It is possible that we could eliminate particular permutations that produce isotopic diagrams.

**Example 5.2.** For example, the permutations $\phi = (4312)$ and $\sigma = (1234)$ create the same right angle diagram as the permutations $\phi' = (2134)$ and $\sigma' = (1432)$, but when we draw them, they are drawn with opposite orientation shown in Figure 5.2 below with $(\phi, \sigma)$ on the left, and $(\phi', \sigma')$ on the right.

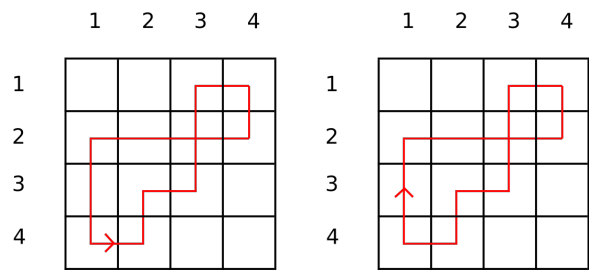


Figure 5.2: Sets of permutations that give opposite orientated diagrams.

We know that there always exists a permutation of each $\phi$ and $\sigma$ as in the previous example because as in our theorem below we know we can always find a pair of permutations that corresponds to the given right angle diagram.

Next we began asking questions about these permutations. For instance, is the map from $(S_{n-1} \times S_n) \to \{\text{RAD}\}$ a bijection? Can we find a generalization of permutations that generate right angle diagrams that are the same, but are oriented differently? What types of permutations give us maximal and minimal crossing number given $t$ turns? Is there a particular feature in the set of permutations that indicates a crossing? In asking these questions, we were able to show the following theorem.

**Theorem 5.1.** *Given $(\phi, \sigma) \in (S_k \times S_{k-1})$ we can produce a right angle diagram. Conversely, given a right angle diagram with orientation and a starting point in the first column, we can find a pair of permutations that corresponds to the given right angle diagram.*

*Proof.* To prove the former statement consider $(\phi, \sigma) \in (S_k \times S_{k-1})$ such that $\sigma = (1, \sigma_2, \cdots, \sigma_{k-1})$, and $\phi = (\phi_1, \phi_2, \cdots, \phi_k)$. Then we have turns at the following set of coordinate pairs

$$(\phi_1, 1)(\phi_1, \sigma_2), (\phi_2, \sigma_2) \cdots, (\phi_k, 1)(\phi_1, 1).$$

Note that we begin and end with the same coordinate pair, so we are guaranteed

to create a closed curve. Also note that each coordinate pair alternately holds the vertical coordinate or the horizontal coordinate constant; this creates the vertical and horizontal segments of our diagram. This guarantees that we will always have only vertical and horizontal lines connecting our $\pm\frac{\pi}{2}$ radian turns, so we have thus shown that our pair of permutations will create a right angle diagram.

Now to prove the later statement consider a right angle diagram with orientation and a starting point. We utilize the starting point of the diagram to produce the first coordinate pair. Given the curve's orientation follow it to our next turn. Write the coordinates of this turn as our next coordinate pair. Proceed in this way until we can record all of the coordinate pairs in order back to the first one. Then write $\sigma$ and $\phi$ from our set of coordinate pairs by recording all of our distinct column and row coordinates. Now we have generated $\sigma$ and $\phi$ from our right angle diagram. □

## 5.2 Grid diagrams and arc presentations

After developing right angle diagrams, we learned that his effort had independently produced a slight generalization of grid diagrams. (See Definition 15 in Chapter 2). There are only two slight differences between right angle diagrams and grid diagrams. First, right angle diagrams do not give crossing information; second grid diagrams utilize $X$'s and $O$'s to describe the turn tiles; right angle diagrams do not. Like right angle diagrams grid diagrams are also oriented, include links, and have only vertical and horizontal strands connecting the turn tiles or $X$'s and $O$'s respectively.

For links, grid diagrams are in correspondence with arc presentation, and have gained popularity recently because of their application to knot Floer homology [7]. Late in this section we show that grid diagrams are directly analogous to the arc presentation of a knot. Our definitions for arc presentation and arc index are given by [3].

**Definition 23.** *An* open-book decomposition *is a decomposition of a closed oriented 3-manifold $M$ into a union of surfaces with boundary and solid tori.*

**Definition 24.** *An* arc presentation *of a link $L$ is an embedding of $L$ in finitely many pages of an open-book decomposition so that each of these pages meets $L$ in a single simple arc. The open-book decomposition separates each arc of the knot onto an individual page, and all of the pages meet at the vertical axis.*

**Definition 25.** Arc index *of a link is the minimum number of pages required to present a given link, denoted $\alpha(L)$.*

Definition 25 partially gives us the correspondence between arc presentation and grid diagrams. The arc index corresponds to the number of vertical strands in our grid diagram. Because the grid diagram is defined so that there is one vertical strand in each column the arc index and the grid index will be equal. We will show that there is total correspondence between the two by projecting our arc presentation onto a cylinder that is centered along the axis of the pages; then we unroll the cylinder to give our grid diagram. The specifics of this process are as follows; we follow the description from [2].

**Theorem 5.2.** *Begin with an arc presentation of a link $L$, and two cylinders $C_1$ and $C_2$ about the axis of the pages of the diagram. Let $C_1$ have radius one, and $C_2$ have radius two. Let each page be labeled from $\{1, 2, \cdots, m\}$, with each page being $\{\theta_1, \cdots, \theta_m\}$ radians apart. Given these tools we will show that the arc presentation and grid diagram of a link $L$ are the same.*

*Proof.* 1. We begin by projecting each arc, $a_i$ that connects an $x_i$ and a $y_i$. $x_i$ and $y_i$ are the positions along the axis where the arcs touch the axis. Each arc will have one $x_i$ and one $y_i$ where $x_i$ is the lowest position of the arc, and $y_i$ is

the highest. This is shown on the left side of Figure 5.3. We project $x_i$ and $y_i$ together onto the surface of $C_2$. We are left with an open 3-gon with vertices $(0, x_i), (0, y_1), (2, x_i), (2, y_i)$, each of these vertices are given by $(r, z)$ where $r$ is the radius and $z$ is the vertical position on the $z$ axis. The segments that are projected onto the cylinder will be the vertical segments of the grid diagram. A diagram of this process is shown below in Figure 5.4.

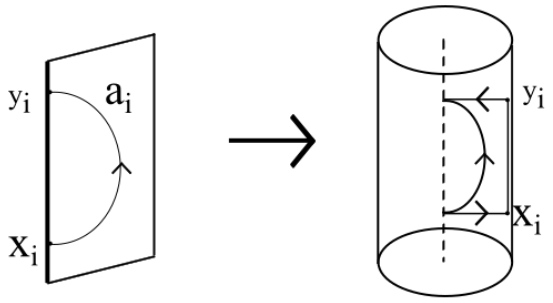


Figure 5.3: The arc $a_i$ being projected onto $C_2$ about the axis of the pages.

2. We have translated the vertical section of each arc, but the arcs are still attached to the axis by the wedge formed by the two half spokes of radius one. This wedge is formed by segments of arcs on adjacent pages, and is attached to the axis at the $(0, z)$ where $z$ is one of our $x_i$'s or $y_i$'s. The half spokes we refer to reach from the axis to the cylinder of radius one, this is the part we pull off of the axis and project onto $C_1$. We do this at each level along the axis. These segments will make up the horizontal components of the diagram. A diagram of the half spokes being projected to $C_1$ is shown below.

3. Now $L$ lies only on $C_1$ and $C_2$ so we can cut the two cylinders along any half plane between pages of the arc presentation. This will give us a trapezoid with height one, a top of width $4\pi$, a base of width $2\pi$ with. We find $m$ levels between the base and the top, one level per page of the arc presentation. The levels represent the points at which the vertical and horizontal strands meet, we

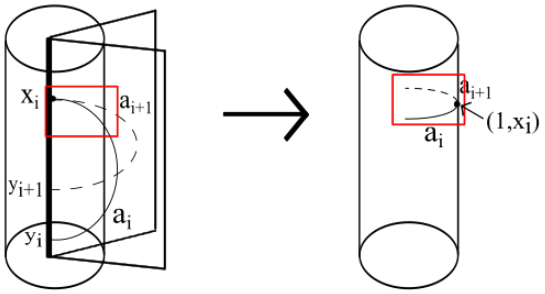


Figure 5.4: Translating the half spokes of radius one at $x_i$ onto $C_1$.

stretch the points out as we separate $C_1$ and $C_2$. The diagram of the trapezoid is shown below.

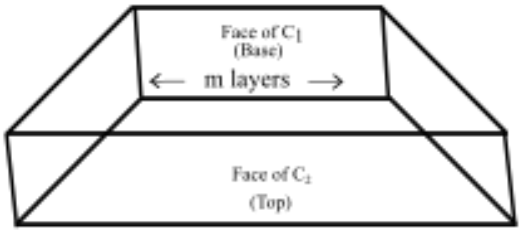


Figure 5.5: Trapezoid made when we cut between two half planes.

4. We then stretch out the face of $C_1$ so that it has length $4\pi$ giving us a rectangular prism. Then looking perpendicularly at what used to be the faces of $C_1$ and $C_2$ we can see the horizontal and vertical strands. These strands come together where the $m$ layers connecting the vertical and horizontal were. We no longer see them because we are looking parallel, down their length. These points become our $X$'s or an $O$'s from our grid diagrams.

□

**Example 5.3.** The following example is for the figure-eight knot, and shows the process of going from a grid diagram to an arc presentation. Beginning with a $5 \times 5$ grid diagram of $4_1$, we draw our vertical components on the face of $C_2$, and draw our

horizontal components on $C_1$; we depict these drawn on the trapezoid. Our five layers connecting them were previously our $X$'s and $O$'s. The horizontal strands are pushed back to the axis of the open-book decomposition where they come to a point. This point will be one of the $x_i$'s or $y_i$'s we talked about in the first step of our algorithm. The vertical strands can now be mapped to the pages of the arc presentation.

Starting from our arc presentation, we would follow the steps described above to generate our vertical and horizontal strands. Our vertical and horizontal strands would then define our grid diagram.

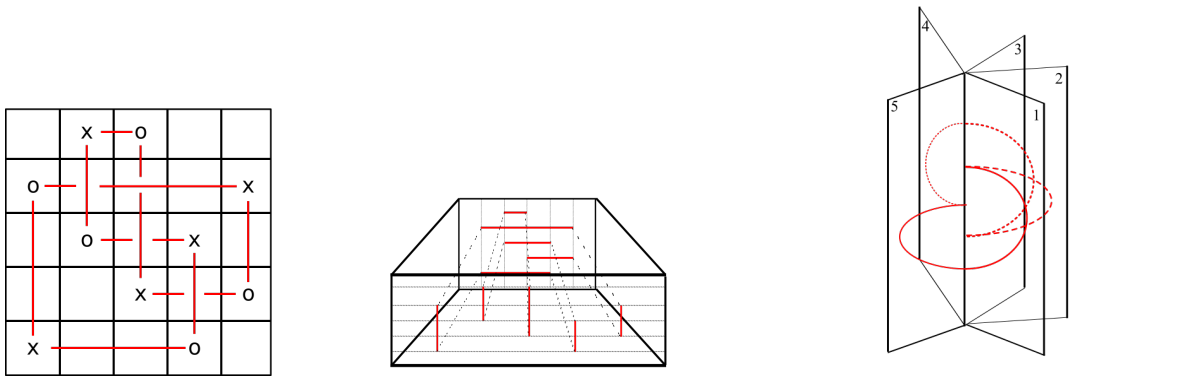


(a) Grid diagram of $4_1$. (b) Applying vertical and horizontal arcs onto the two cylinders. (c) Projecting onto the pages of the arc presentation.

Figure 5.6: Grid diagram to arc presentation.

# Bibliography


[1] Adams, Colin C. *The Knot Book.* W. H. Freeman and Company, New York, 1994.

[2] Arbel, Julyan. *Arc presentation of knots and links.* Masters Thesis. University of Liverpool. 2006.

[3] Cromwell, Peter R. *Knots and Links.* Cambridge University Press, Cambridge, 2004.

[4] Irina T. Garduno. *"Virtual Mosaic Knots." Rose-Hulman Undergraduate Mathematics Journal*, Vol. 10. 2009. Issue 2.

[5] Hwa Jeong Lee, Lewis D Ludwig, Joseph S. Paat, Amanda Peiffer. *"Knot Mosaic Tabulation."* arXiv:1602.03733

[6] Lomonaco, Samuel J.; Kauffman, Louis H. "Quantum knots and mosaics." *Quantum information science and its contributions to mathematics,* Proc. Sympos. Appl. Math., 68, Am Math Sec.

[7] Ng, Lenhard; Thurston, Dylan. "Grid diagrams, braids, and contact geometry." *Proceedings of Gkova Geometry-Topology Conference 2008,*

**Curriculum Vitae : Sarah Roberts**


# Sarah Roberts

*saraheroberts17@gmail.com*

3985 Shattalon Drive
Winston Salem, NC 27106

(770) 329-9489 [Cell]


## Education

**Wake Forest University** — Winston Salem, North Carolina

Masters in Mathematics — Expected May 2017

**Berry College** — Mount Berry, GA

Bachelor of Science in Mathematics — May 2015

Minor in Chemistry

## Work Experience

**Teaching Assistant** — August 2015 – May 2017

Wake Forest University Mathematics — Supervisor: Dr. Ellen Kirkman

**Math Center Tutor** — May 2016 – July 2016

Wake Forest University Mathematics — Supervisor: Mrs. Jule Connolly

**Private Tutor** — June 2016 –Present

Julie Fuller — (336) 407-8221

Rebekah Harmon — (336) 391-3952

Kim Morgan — (336) 682-5085

**Applied Calculus Tutor** — August 2014 – May 2015

Berry College Math and Computer Science — Supervisor: Dr. Zahava Wilstein

**Math Lab Tutor** August 2013 – May 2015

Berry College Math and Computer Science Supervisor: Dr. Ron Taylor

**Multivariable Calculus Grader** January 2014 – May 2015

Berry College Math and Computer Science Supervisor: Dr. Ron Taylor

## Activities

| | |
|---|---|
| IMMERSE at University of Nebraska, Lincoln | June 2015 – July 2015 |
| Dead Poets Society (Berry College Math Club) | August 2013 – May 2017 |
| Berry College Symphony Orchestra | August 2011 – May 2017 |
| Winshape College Program | August 2012 – May 2017 |
| Virginia Tech Regional Mathematics Contest | 2013, 2014 |
| William Lowell Putnam Mathematical Competition | 2013, 2014 |

## Research Experience

**Wake Forest University** Winston Salem, NC

Finding Bounds on Crossing number for Mosaic Diagrams of Knots May 2016 – present

This research project focuses on my masters thesis work done with Dr. Jason Parsley. The project is centered about the subject of knot mosaics and their relations to other knot invariants. We have proven relationships

between crossing number and winding number of knots. We are restricting our relation to the case of mosaic diagrams of knots.

**Berry College** Mount Berry, GA

Modeling With Differential Equations August 2014 – May 2017

Research assistant for Dr. Zahava Wilstein. We began our work by researching methods for modeling systems in vivo with differential equations. As our research continued, I led a team of other research students in writing differential equations to describe vascular remodeling in the human body, and ran differential equations through Mathematica to refine our system of ODEs. We also worked with a team of biologists to research the system to find better ways to write ODEs.

Sequence of Circles and Polygons August 2013 – April 2014

Worked with Dr. Ron Taylor on a question posed to him at a mathematics conference. We began with a circle of radius r and inscribed an equilateral triangle in it, then we continued the sequence by alternately inscribing a circle and a regular polygon with one more edge than the previous polygon. Next we investigated whether there was a limiting circle of a positive radius, or if the construction collapsed to a point. We discovered that there was a limiting circle, and found the length of the radius that the sequence converged to when the radius of the initial circle had the length of one unit.

## Scholarships

**Wake Forest University** Winston Salem, NC

Teaching Assistantship August 2015 – May 2017

**Berry College** Mount Berry, GA

| | |
|---|---|
| Winshape College Program | August 2012 – May 2014 |
| Berry Music Scholarship | August 2011 – May 2014 |
| Berry College Dean's Scholarship | August 2011 – May 2014 |
| Berry College Academic Scholarship | August 2011 – May 2014 |
| Georgia Hope Scholarship | August 2011 – May 2014 |

## Presentations

- *A Mathematical Description of Vascular Remodeling*, Spring 2015 Berry College Symposium, Mount Berry, Ga, April 2015.
- *On Inscribing A Sequence of Polygons in a Circle*, Spring 2014 MAA Section Meeting, Cookeville, TN, March 2014.
- *On Inscribing A Sequence of Polygons in a Circle*, Spring 2014 Berry College Symposium on Student Scholarship, Mount Berry, GA, April 2014.

## Recognitions

- Barton Mathematics Award, Spring 2015
- Berry College Student Work Certificate, Spring 2015
- Berry College Symphony Orchestra Concertmaster, Fall 2014
- Dean's List, Fall 2013 and Fall 2014
- First Year Council, 2011

## Service

**Wake Forest University Mathematics** January 2016 – Present

Paisley IB Magnet Mathematics Enrichment Program

- Volunteer for and organize an enrichment program for middle school students at Paisley IB Magnet School in Winston Salem. Graduate students from Wake Forest University's Department of Mathematics work with participating Paisley students on challenging, fun, and engaging math problems and games. The goals for this time include furthering the students' critical thinking skills as well as deepening their appreciation for mathematics.

**Winshape College Program** August 2014 – May 2015

301A Community Impact Team

- Helped create the "301A Community Impact Team" through the Winshape College Program. 301A met three times a week to read to or tutor elementary through middle-school-aged kids.

**Friends of Refugees** May 2012 – August 2012

- Counselor for a camp created to serve the refugee children in the community of Clarkston, Georgia. Worked with middle school girls as a counselor, and helped plan camp events such as block parties, field trips, and lesson plans.

# References

**Dr. Jason Parsley**

Department of Mathematics

Wake Forest University

127 Manchester Hall

PO Box 7388

Winston-Salem, NC 27109

rparslerj@wfu.edu

Relationship: Professor for two years, thesis advisor.

**Mrs. Jule Connolly**

Department of Mathematics

Wake Forest University

127 Manchester Hall

PO Box 7388

Winston-Salem, NC 27109

(336) 758-6094

connolly@wfu.edu

Relationship: Supervisor for one year.

**Dr. Ron Taylor**

Department of Mathematics

Berry College

2277 Martha Berry Hwy

P.O Box 5014

Mount Berry, GA 30149

(706) 290-2677

rtaylor@berry.edu

Relationship: Professor for three years, work supervisor, research supervisor, and mentor for two years.